

## **Supporting Information**

# **Cheap, Large-scale, and High-performance Graphite-based Flexible Thermoelectric Materials and Devices with Supernormal Industry Feasibility**

*Shuai Sun,<sup>†</sup> Xiao-Lei Shi,<sup>†,‡</sup> Wei-Di Liu,<sup>†</sup> Ting Wu,<sup>※</sup> Dezhuang Wang,<sup>※</sup> Hao Wu,<sup>※</sup> Xiaoyong Zhang,<sup>□</sup> Yu Wang,<sup>§</sup> Qingfeng Liu,<sup>※\*, \*</sup> and Zhi-Gang Chen<sup>†,‡, \*</sup>*

<sup>†</sup>*Centre for Future Materials, University of Southern Queensland, Springfield Central, Queensland 4300, Australia.*

<sup>‡</sup>*School of Chemistry and Physics, Queensland University of Technology, Brisbane City QLD 4000, Australia.*

<sup>※</sup>*State Key Laboratory of Materials Oriented Chemistry Engineering, College of Chemistry Engineering, Nanjing Tech University, Nanjing 211800, China.*

<sup>□</sup>*School of Materials Science and Engineering, Anhui University of Science and Technology, Huainan 232001, China.*

<sup>§</sup>*Jiangxi Bluestar Xinghuo Silicone Co., Ltd., Jiujiang 330319, China.*

*Correspondence should be addressed at:*

*\*E-mail: [qfliu@njtech.edu.cn](mailto:qfliu@njtech.edu.cn) and [zhigang.chen@usq.edu.au](mailto:zhigang.chen@usq.edu.au)*

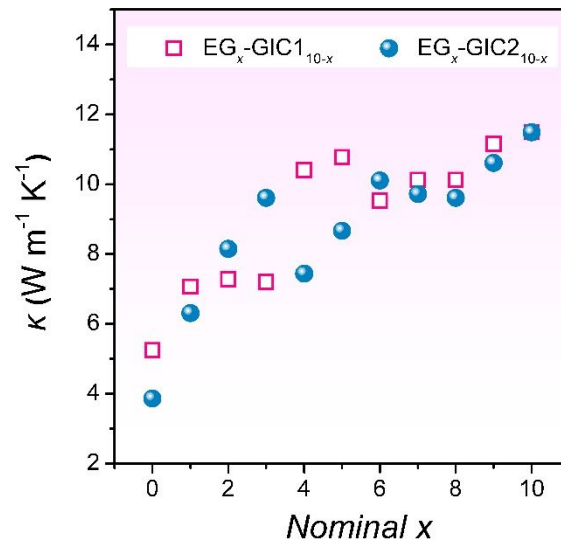


**Figure S1.** Vertical thermal conductivities of the as-prepared composites.

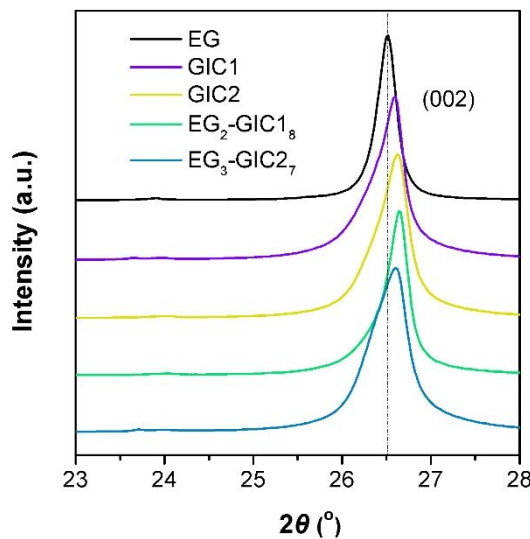


**Figure S2.** Enlarged XRD spectra highlighting the (002) diffraction peaks.

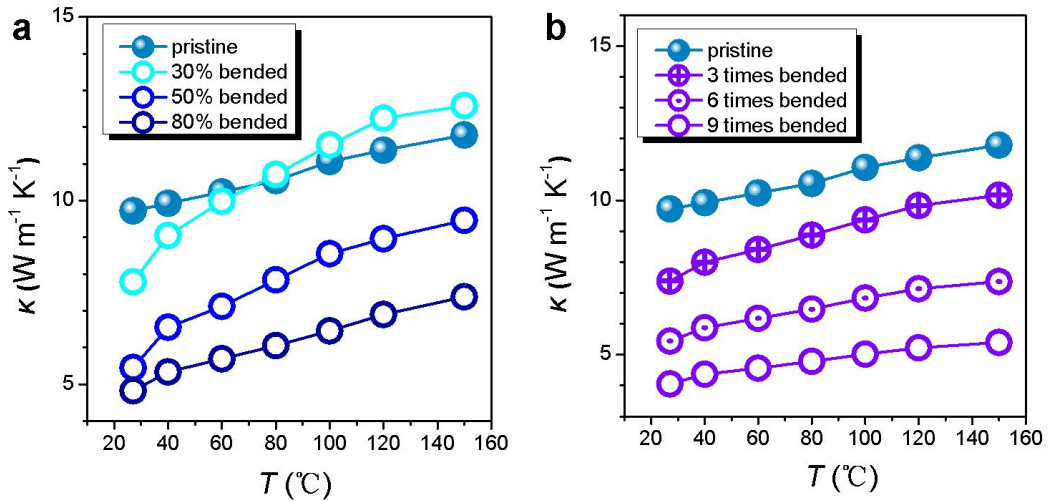


**Figure S3.** Thermal conductivities of  $\text{EG}_3\text{-GIC2}_7$  films as a function of temperature.

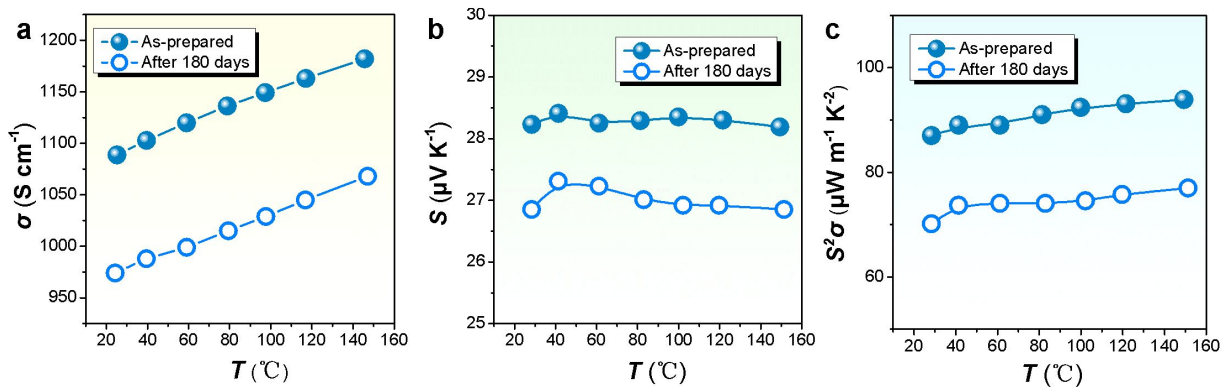


**Figure S4.** (a)  $\sigma$ , (b)  $S$ , and (c)  $S^2\sigma$  of  $\text{EG}_3\text{-GIC2}_7$ , under as-prepared status and after exposed in the air for 180 days.

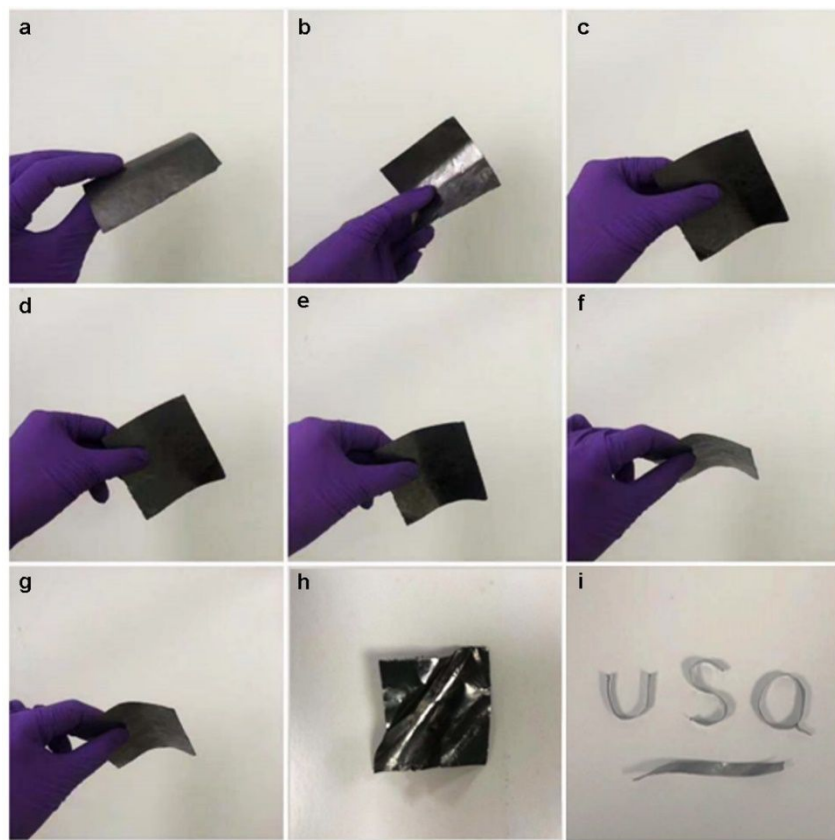


**Figure S5.** Arbitrary shaping images of EG<sub>3</sub>-GIC2<sub>7</sub>.

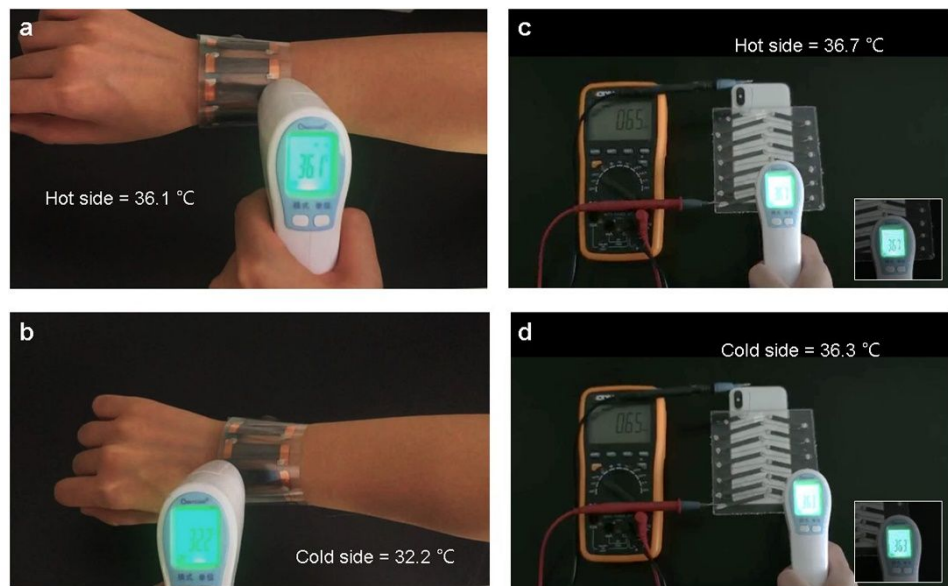


**Figure S6.** Temperature measurement of the hot side and cold side in conditions of (a-b) Human body as the heat source, and (c-d) Cellphone back shell as the heat source.

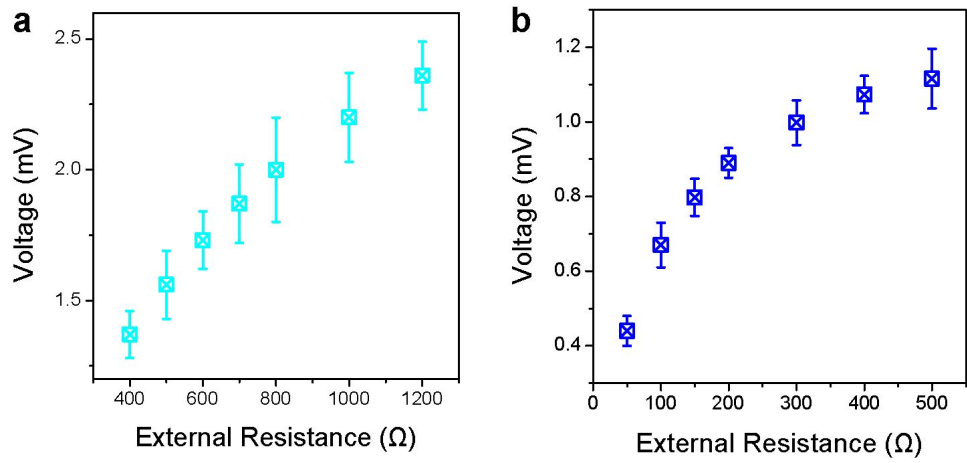


**Figure S7.** The voltage on the external variable resistor as a function of external resistance of (a) Device-1, and (b) Device-2.

**Table S1.** Comparison of thermoelectric properties and prices of the as-prepared composite EG<sub>3</sub>-GIC<sub>7</sub> and some typical flexible thermoelectric materials reported in literature.

Materials	Filler/adhesive	Loading (wt.%)	Form	Type	T (K)	$\sigma$ (S cm <sup>-1</sup> )	S ( $\mu$ V K <sup>-1</sup> )	$S^2\sigma$ ( $\mu$ W m <sup>-1</sup> K <sup>-2</sup> )	$\kappa$ (W m <sup>-1</sup> K <sup>-1</sup> )	ZT	Price (\$ g <sup>-1</sup> )	ref
This work			flexible	p	300	1089	28.2	87	-	-	0.012	
PEDOT			flexible	p	300	23	12.9	39	-	-	-	(S1)
PEDOT:PSS			flexible	p	300	453	23.1	24	-	-	117	(S2)
P3HT			flexible	p	300	250	40	38	~0.18	~0.06	188	(S3)
PANI			flexible	p	300	12.5	11	0.2	-	-	76	(S4)
Graphite			solid	p	298	1400	5	3.5	-	-	0.008	(S5)
Expanded graphite			flexible	P	300	1000	10.4	11	-	-	0.014	(S6)
Carbon fiber	Sulfate–aluminate cement	0.5	solid	p	329	-	-	2	-	0.003	0.023	(S7)
Expanded graphite	PC	50	flexible	p	300	~11.4	~26	~0.8	-	-	0.009	(S8)
Expanded graphite	PEDOT:PSS	20	flexible	p	298	213	16	5.3	-	~2.3*10 <sup>-4</sup>	23	(S9)
Expanded graphite	PVA/PEI	60/20	flexible	n	300	10	-25.3	0.6	~0.3	~6*10 <sup>-4</sup>	0.006	(S10)
Expanded graphite	ionic liquid/Sulfate–aluminate cement	3/90	solid	n	308 345	~0.003 ~3	~150 -568	~0.67 94	3.296	2.06*10 <sup>-3</sup>	1.25	(S11)
PEDOT	rGO	17	flexible	p	300	516	16	13	-	-	-	(S12)
PEDOT:PSS	Ca <sub>3</sub> Co <sub>4</sub> O <sub>9</sub>	10	flexible	P	300	135	18.1	4	-	-	-	(S13)
PEDOT:PSS	Sb <sub>2</sub> Te <sub>3</sub>	-	flexible	P	300	341	92.6	292	0.44	0.2	-	(S14)
PEDOT:PSS	SnSe	20	flexible	p	300	320	110	387	0.36	0.32	-	(S15)
PEDOT:PSS	Te NWs	7	flexible	P	300	19.3	163	51	0.22	0.1	-	(S16)
PEDOT:PSS	Te NWs	-	flexible	p	300	215	115	284	0.22	0.39	-	(S17)

PEDOT:PSS	SWCNTs	85	flexible	P	300	3300	20	132	0.45-0.69	0.03	-	(S18)
PEDOT:PSS	Bi <sub>2</sub> Te <sub>3</sub>	10	flexible	n	300	55	-110	67	0.558	0.04	-	(S19)
P3HT	Te NWs	25	flexible	p	300	-	285	-	-	-	-	(S20)
P3HT	Bi <sub>2</sub> Te <sub>3</sub> NWs	15	flexible	P	300	11.23	110	14	0.75	-	-	(S21)
PANI	Graphene	50	flexible	p	300	123	34	14	0.46	-	-	(S22)
CNTs	PANI	15.8	flexible	p	300	61.47	28.6	5	0.50	0.003	-	(S23)
CNTs	PEDOT:PSS	65	flexible	P	300	380	27	25	0.34	0.02	-	(S24)
CNTs	PDMS	60	flexible	p	300	68	51	18	-	0.0039	-	(S25)
SWCNTs	PANI	58.6	flexible	P	300	125	40	20	1.5	0.004	-	(S26)
SWCNTs	PEDOT:PSS	50	flexible	p	300	900	30	84	-	-	-	(S27)
SWCNTs	PPy	60	flexible	P	300	400	22	20	-	-	-	(S28)
Graphene	PANI	55	flexible	p	300	856	15	19	-	-	-	(S29)
Graphene	PEDOT:PSS	97	flexible	P	300	637	26.8	45.7	-	-	-	(S2)
RGO	PEDOT:PSS	97	flexible	p	300	1160	17	32.6	-	-	-	(S30)

**Table S2.** Preliminary experiment results of thermoelectric properties of different as-prepared commercial-carbon based composite materials.

Samples composition <sup>a</sup>	$\sigma$ (S cm <sup>-1</sup> )	$S$ ( $\mu$ V K <sup>-1</sup> )	$S^2\sigma$ ( $\mu$ W m <sup>-1</sup> K <sup>-2</sup> )
EG (12 MPa 5min) <sup>b</sup>	1017	13.4	18.26
EG (13.5 MPa 10min) <sup>b</sup>	534	12.4	8.21
Commercial Graphite Paper <sup>c</sup>	870	6.85	4.08
34% EG + 60% GIC1	1214	23.48	66.9
34% EG powder + 60% GIC1	985	23.51	54.44
34% EG powder + 60% GIC1 + 6% PF	419	19.1	15.29
34% NG powder + 60% GIC1 + 4% PF + 2% PVB	531	19.7	20.6
EG powder	692	13.9	13.37
34% NG powder + 60% GIC1 + 6% PPS	218	20.1	8.81
60% NG powder + 34% GIC1 + 6% PF	431	20.5	18.11
60% NG powder + 34% GIC1 + 6% PVDF	104	26.2	7.14
34% NG powder + 60% GIC1 + 6% PVDF	40	25.5	2.6
34% NG powder + 60% GIC1 + 6% PF	246.2	18.02	7.99
30% GIC1 + 15% NG powder + 49% CB + 6% PF	124	10.9	1.47
60% GIC1 + 34% NG powder + 6% PBA	166	21.4	7.6
60% GIC1 + 34% NG powder + 4% PBA + 2% PVB	316	23.1	16.86
50% EG + 42.5% CB + 6% PF	281	8.5	2.03
94% EG + 6% PF	796	11.4	10.34
60% EG + 34% GIC1 + 6% PF	830	14	16.27
60% EG + 34% NG powder + 6% PF	802	12.6	12.73
34% EG + 60% NG powder + 6% PF	600	11.7	8.21
45% GIC1 + 25% NG powder + 20% CB + 10% PF	581	15.5	13.96
60% NFG1 + 34% NG powder + 6% PF	698	9.6	6.43
60% NFG2 + 34% NG powder + 6% PF	1039	10.5	11.45
60% GIC1 + 34% NG powder + 6% PF	450	17.4	13.6
60% GIC2 + 34% NG powder + 6% PF	833	18.12	27.35
78.5% EG + 12% GIC2 + 8% CB + 1.5% PVDF	694	11	8.4
78.5% EG + 12% GIC2 + 8% CB + 1.5% PF	525	11.5	6.94
58.5% EG + 24% GIC2 + 16% NG powder + 1.5% PVDF	884	14.9	19.63
58.5% EG + 24% NG powder + 16% GIC2 + 1.5% PVDF	1019	14.3	20.84
78.5% EG + 12% GIC2 + 8% NG powder + 1.5% PVDF	1012	13.5	18.44
78.5% EG + 12% NG powder + 8% GIC2 + 1.5% PVDF	1174	13	19.84
78.5% EG + 20% GIC2 + 1.5% PVDF	935	11.6	12.58
58.5% EG + 40% GIC2 + 1.5% PVDF	695	11.4	9.03
58.5% EG + 40% GIC2 + 1.5% PF	885	12.1	12.96
58.5% EG + 24% GIC2 + 16% NG powder + 1.5% PF	820	10.2	8.53
58.5% EG + 40% GIC2 + 1.5% PVDF	900	13.8	17.14
58.5% EG + 40% GIC2 + 1.5% PF	550	11.8	7.66

<sup>a</sup> EG powder stands for expanded graphite powder which is 90 mesh before expending, NG powder stands for natural graphite powder, CB stands for carbon black, NFG1 stands for 170 mesh natural

flake graphite, NFG2 stands for 90 mesh natural flake graphite, PVB stands for poly(vinyl butyral), PPS stands for poly(phenylene sulfide), PBA stands for poly(butyl acrylate).

<sup>b</sup> According to the thermoelectric results here, all of the other samples are hot-pressed under the condition of 12 MPa, 5min.

<sup>c</sup> Purchased from Qingdao Dong Kai Carbon Co., Ltd. (Shandong, China) with a thickness of 0.3  $\mu\text{m}$ .

**Table S3.** Preliminary experiment results of thermoelectric properties of the particals with different EG sizes.

Samples composition	$\sigma$ ( $\text{S cm}^{-1}$ )	$S$ ( $\mu\text{V K}^{-1}$ )	$S^2\sigma$ ( $\mu\text{W m}^{-1} \text{K}^{-2}$ )
EG <sub>2</sub> -GIC2 <sub>8</sub> <sup>a</sup>	863	21.6	40.26
EG <sub>4</sub> -GIC2 <sub>6</sub>	1088	25.2	69.91
EG <sub>6</sub> -GIC2 <sub>4</sub>	1209	21.7	56.93
EG <sub>8</sub> -GIC2 <sub>2</sub>	1020	11.2	12.79
EG' <sub>2</sub> -GIC2 <sub>8</sub> <sup>b</sup>	811	21.5	37.49
EG' <sub>4</sub> -GIC2 <sub>6</sub>	990	24.6	59.91
EG' <sub>6</sub> -GIC2 <sub>4</sub>	1021	21.5	47.20
EG' <sub>8</sub> -GIC2 <sub>2</sub>	1102	13.8	20.99

<sup>a</sup> EG stands for expanded graphite powder which is 90 mesh before expending, GIC1 stands for 170 mesh graphite intercalation on compounds powder.

<sup>b</sup> EG' stands for expanded graphite powder which is 50 mesh before expending, GIC1 stands for 170 mesh graphite intercalation on compounds powder.

**Table S4.** Detailed XRD characteristic wavenumbers, integral areas and  $I_D/I_G$  values of EG, GIC1, GIC2, EG<sub>2</sub>-GIC1<sub>8</sub> and EG<sub>3</sub>-GIC2<sub>7</sub>.

Samples	D band		G band		G' band		$I_D/I_G$
	Wavenumber ( $\text{cm}^{-1}$ )	Integral area	Wavenumber ( $\text{cm}^{-1}$ )	Integral area	Wavenumber ( $\text{cm}^{-1}$ )	Integral area	
EG	1345	426.5	1580	9170.3	2719	9089.4	0.047
GIC1	1354	557.2	1580	8367.1	2724	7602.5	0.067
GIC2	1359	535.1	1580	8570.8	2720	8251.2	0.062
EG <sub>2</sub> -GIC1 <sub>8</sub>	1352	987.6	1580	10420.4	2720	9987.7	0.095
EG <sub>3</sub> -GIC2 <sub>7</sub>	1354	786.8	1580	8340.3	2721	8113.6	0.094

**Table S5.** Detailed element content ratios of EG, GIC1, GIC2, EG<sub>2</sub>-GIC1<sub>8</sub>, and EG<sub>3</sub>-GIC2<sub>7</sub> provided by XPS measurements.

Samples	C1s content (%)	N1s content (%)	O1s content (%)	S2p content (%)
EG	96.57	0.56	2.68	0.19
GIC1	71.62	4.42	19.41	4.55
GIC2	75.55	3.94	16.83	3.68
EG <sub>2</sub> -GIC1 <sub>8</sub>	94.54	1.02	3.93	0.50
EG <sub>3</sub> -GIC2 <sub>7</sub>	96.68	0.67	2.42	0.23

**Table S6.** Thermoelectric properties of EG<sub>3</sub>-GIC2<sub>7</sub> films after different bending cycles.

EG <sub>3</sub> -GIC2 <sub>7</sub> bending cycles	$\sigma$ (S cm <sup>-1</sup> )	$S$ ( $\mu$ V K <sup>-1</sup> )	$S^2\sigma$ ( $\mu$ W m <sup>-1</sup> K <sup>-2</sup> )
pristine	1089	28.2	86.60
1	1238	25.6	81.13
2	1058	26.2	72.63
3	995	27.1	73.07
4	989	27.6	75.34
5	1107	25.6	72.55
6	996	26.3	68.89
7	989	27.2	73.17
8	998	26.4	69.56
9	986	26.9	71.35
10	967	27.4	72.60

**Table S7.** Thermal conductivities of EG<sub>3</sub>-GIC2<sub>7</sub> films after different bending ratios and bending cycles.

Bending ratios (%)	$\kappa$ <sup>a</sup> (W m <sup>-1</sup> K <sup>-1</sup> )	Bending cycles <sup>b</sup>	$\kappa$ (W m <sup>-1</sup> K <sup>-1</sup> )
0	9.72	0	9.72
10	8.40	1	7.79
20	7.57	2	7.23
30	7.79	3	7.38
40	6.10	4	6.51
50	5.45	5	5.97
60	5.33	6	5.44
70	5.36	7	6.12
80	4.82	8	4.78
-	-	9	4.05
-	-	10	3.65

<sup>a</sup> Calculated by the formula of  $\kappa = D \times C_p \times \rho$ , where  $D$  is the thermal diffusivity coefficient,  $C_p$  is the specific heat capacity.  $D$  was measured by a laser flash method (LFA 467, NETZSCH, Germany).  $C_p$  was measured by differential scanning calorimetry (DSC, NETZSCH STA 449F3).

<sup>b</sup> Bending ratios of all cycles were kept at 30 % where thermal diffusivity coefficients were measured with unrolled samples after described bending cycles.

**Table S8.** Hall coefficients and carrier concentrations  $n$  of EG<sub>3</sub>-GIC<sub>2</sub><sub>7</sub> films after different bending cycles.

Bending cycles <sup>a</sup>	Hall coefficient <sup>b</sup> (m <sup>3</sup> C <sup>-1</sup> )	$n$ <sup>c</sup> ( $\times 10^{20}$ m <sup>-3</sup> )
0	0.04128	1.5141
1	0.04096	1.5257
2	0.04198	1.4889
3	0.04168	1.4995
4	0.04138	1.5103
5	0.04087	1.5293
6	0.04210	1.4845
7	0.04163	1.5012
8	0.04108	1.5216
9	0.04066	1.5373
10	0.04123	1.5159

<sup>a</sup> Bending ratios of all cycles were kept at 30 % where Hall effects were measured with unrolled samples after described bending cycles.

<sup>b</sup> Measured by the Van der Pauw method (F-50, CH-Hall Electronic, China).

<sup>c</sup> Calculated using  $n=1/(eR_H)$ , where  $e$  represents the electron charge and  $R_H$  represents the Hall coefficient.

**Table S9.** The open-circuit voltage of Device-1 after different bending ratios and bending cycles.

Bending ratios (%)	Average open-circuit voltage (mV)	20 times fluctuation range <sup>a</sup> (mV)	Bending cycles <sup>b</sup>	Open-circuit voltage (mV)	20 times fluctuation range (mV)
0	3.72	3.32~4.08	0	3.72	3.22~4.18
10	3.56	3.28~3.97	1	3.71	3.24~4.00
20	3.63	3.25~4.02	2	3.74	3.12~4.19
30	3.67	3.22~4.12	3	3.65	3.05~4.13
40	3.62	3.17~4.17	4	3.67	3.13~4.21
50	3.58	2.95~4.08	5	3.70	3.01~4.27
60	3.65	2.81~4.37	6	3.62	2.88~4.29
70	3.52	2.70~4.35	7	3.57	2.83~4.16
80	3.47	2.68~4.46	8	3.64	2.96~4.22
-	-	-	9	3.61	2.85~4.38
-	-	-	10	3.56	2.76~4.01

<sup>a</sup> Open-circuit voltage fluctuation range among 20 times' measurements.

<sup>b</sup> Bending ratios of all cycles were kept at 30 %.

**Table S10.** The open-circuit voltage of Device-2 after different bending ratios and bending cycles.<sup>a</sup>

Bending ratios (%)	Average open-circuit voltage (mV)	20 times fluctuation range <sup>b</sup> (mV)	Bending cycles <sup>c</sup>	Average open-circuit voltage (mV)	20 times fluctuation range (mV)
0	1.31	0.94~1.67	0	1.31	0.94~1.67
10	1.33	1.02~1.65	1	1.30	0.91~1.63
20	1.29	1.02~1.72	2	1.33	0.88~1.56
30	1.30	0.96~1.63	3	1.27	0.90~1.66
40	1.28	0.91~1.60	4	1.29	0.93~1.69
50	1.29	0.96~1.65	5	1.30	0.99~1.71
60	1.26	0.89~1.63	6	1.27	0.85~1.60

70	1.29	0.95~1.59	7	1.31	1.04~1.70
80	1.27	0.87~1.61	8	1.28	0.88~1.59
-	-	-	9	1.26	0.91~1.67
-	-	-	10	1.29	0.86~1.64

<sup>a</sup> Tests were conducted in the scene of submerging in the river water as cold side ( $\Delta T = 1.6 \text{ }^{\circ}\text{C}$ ).

<sup>b</sup> Open-circuit voltage fluctuation range among 20 times' measurements.

<sup>c</sup> Bending ratios of all cycles were kept at 30 %.

**Table S11.** Thermoelectric properties and thicknesses of EG<sub>3</sub>-GIC2<sub>7</sub> films with different pressing pressures and pressing times.

EG <sub>3</sub> -GIC2 <sub>7</sub> pressing method	$\sigma$ (S cm <sup>-1</sup> )	S ( $\mu\text{V K}^{-1}$ )	$S^2\sigma$ ( $\mu\text{W m}^{-1} \text{K}^{-2}$ )	Thickness (mm)
8 MPa	709	23.9	40.50	0.34
10 MPa	940	24.5	56.40	0.31
12 MPa	1089	28.2	86.60	0.32
15 MPa	982	25.8	65.37	0.30
15 MPa, 1 time <sup>a</sup>	1089	28.2	86.60	0.32
15 MPa, 3 time	1230	24.9	76.26	0.30
15 MPa, 5 time	1138	24.5	68.31	0.25
15 MPa, 7 time	1091	21.2	49.03	0.23

<sup>a</sup> 5 min for each time.

**Table S12.** Sizes of the samples corresponding to the measurement of the thermoelectric performances.<sup>a</sup>

Samples	Length (mm)	Width (mm)	Thickness (mm)
EG	22.13	7.91	0.31
GIC1	21.02	7.37	0.30
GIC2	22.89	7.58	0.30
EG <sub>1</sub> -GIC1 <sub>9</sub>	21.68	7.97	0.28
EG <sub>2</sub> -GIC1 <sub>8</sub>	22.10	7.62	0.30
EG <sub>3</sub> -GIC1 <sub>7</sub>	21.53	7.32	0.27

EG <sub>4</sub> -GIC1 <sub>6</sub>	21.95	7.59	0.28
EG <sub>5</sub> -GIC1 <sub>5</sub>	22.64	7.44	0.31
EG <sub>6</sub> -GIC1 <sub>4</sub>	21.72	7.48	0.30
EG <sub>7</sub> -GIC1 <sub>3</sub>	22.55	7.27	0.31
EG <sub>8</sub> -GIC1 <sub>2</sub>	21.96	7.73	0.32
EG <sub>9</sub> -GIC1 <sub>1</sub>	22.12	7.30	0.31
EG <sub>1</sub> -GIC2 <sub>9</sub>	22.02	7.85	0.31
EG <sub>2</sub> -GIC2 <sub>8</sub>	21.87	7.46	0.28
EG <sub>3</sub> -GIC2 <sub>7</sub>	22.77	7.25	0.32
EG <sub>4</sub> -GIC2 <sub>6</sub>	22.60	7.32	0.30
EG <sub>5</sub> -GIC2 <sub>5</sub>	21.82	7.61	0.29
EG <sub>6</sub> -GIC2 <sub>4</sub>	22.35	7.55	0.30
EG <sub>7</sub> -GIC2 <sub>3</sub>	22.33	7.59	0.32
EG <sub>8</sub> -GIC2 <sub>2</sub>	21.92	7.81	0.31
EG <sub>9</sub> -GIC2 <sub>1</sub>	21.75	7.32	0.31

<sup>a</sup> Samples were used for the measurement of the thermoelectric properties shown in **Figures 2a-c**.

## REFERENCES

- (S1) Xu, K.; Chen, G.; Qiu, D. Convenient construction of poly(3,4-ethylenedioxythiophene)-graphene pie-like structure with enhanced thermoelectric performance. *J. Mater. Chem. A* **2013**, *1*, 12395.
- (S2) Yoo, D.; Kim, J.; Kim, J. H. Direct synthesis of highly conductive poly(3,4-ethylenedioxythiophene):poly(4-styrenesulfonate) (PEDOT:PSS)/graphene composites and their applications in energy harvesting systems. *Nano Res.* **2014**, *7*, 717-730.
- (S3) Qu, S.; Yao, Q.; Wang, L.; Chen, Z.; Xu, K.; Zeng, H.; Shi, W.; Zhang, T.; Uher, C.; Chen, L. Highly anisotropic P3HT films with enhanced thermoelectric performance via organic small molecule epitaxy. *NPG Asia Mater.* **2016**, *8*, e292-e292.

- (S4) Reddy, B. N.; Deepa, M.; Joshi, A. G.; Srivastava, A. K. Poly(3,4-Ethylenedioxypyrrole) Enwrapped by Reduced Graphene Oxide: How Conduction Behavior at Nanolevel Leads to Increased Electrochemical Activity. *J. Phys. Chem. C* **2011**, *115*, 18354-18365.
- (S5) Andrei, V.; Bethke, K.; Rademann, K. Adjusting the thermoelectric properties of copper(I) oxide-graphite-polymer pastes and the applications of such flexible composites. *Phys. Chem. Chem. Phys.* **2016**, *18*, 10700-10707.
- (S6) Wei, J.; Zhao, L.; Zhang, Q.; Nie, Z.; Hao, L. Enhanced thermoelectric properties of cement-based composites with expanded graphite for climate adaptation and large-scale energy harvesting. *Energ. Buildings* **2018**, *159*, 66-74.
- (S7) Wei, J.; Zhang, Q.; Zhao, L.; Hao, L.; Yang, C. Enhanced thermoelectric properties of carbon fiber reinforced cement composites. *Ceram. Int.* **2016**, *42*, 11568-11573.
- (S8) Javadi, R.; Choi, P. H.; Park, H. S.; Choi, B. D. Preparation and Characterization of P-Type and N-Type Doped Expanded Graphite Polymer Composites for Thermoelectric Applications. *J. Nanosci. Nanotechnol.* **2015**, *15*, 9116-9119.
- (S9) Culebras, M.; Gómez, C. M.; Cantarero, A. Thermoelectric measurements of PEDOT:PSS/expanded graphite composites. *J. Mater. Sci.* **2012**, *48*, 2855-2860.
- (S10) Piao, M.; Kim, G.; Kennedy, G. P.; Roth, S.; Dettlaff-Weglikowska, U. Preparation and characterization of expanded graphite polymer composite films for thermoelectric applications. *Phys. Status Solidi B* **2013**, *250*, 2529-2534.
- (S11) Wei, J.; Li, X.; Wang, Y.; Chen, B.; Qiao, S.; Zhang, Q.; Xue, F. Record high thermoelectric performance of expanded graphite/carbon fiber cement composites enhanced by ionic liquid 1-butyl-3-methylimidazolium bromide for building energy harvesting. *J. Mater. Chem. C* **2021**, *9*, 3682-3691.
- (S12) Xu, K.; Chen, G.; Qiu, D. In situ chemical oxidative polymerization preparation of poly(3,4-ethylenedioxothiophene)/graphene nanocomposites with enhanced thermoelectric performance. *Chem. Asian J.* **2015**, *10*, 1225-1231.

- (S13) Liu, C.; Jiang, F.; Huang, M.; Lu, B.; Yue, R.; Xu, J. Free-Standing PEDOT-PSS/Ca<sub>3</sub>Co<sub>4</sub>O<sub>9</sub> Composite Films as Novel Thermoelectric Materials. *J. Electron. Mater.* **2010**, *40*, 948-952.
- (S14) We, J. H.; Kim, S. J.; Cho, B. J. Hybrid composite of screen-printed inorganic thermoelectric film and organic conducting polymer for flexible thermoelectric power generator. *Energy* **2014**, *73*, 506-512.
- (S15) Ju, H.; Kim, J. Chemically Exfoliated SnSe Nanosheets and Their SnSe/Poly(3,4-ethylenedioxythiophene):Poly(styrenesulfonate) Composite Films for Polymer Based Thermoelectric Applications. *ACS Nano* **2016**, *10*, 5730-5739.
- (S16) See, K. C.; Feser, J. P.; Chen, C. E.; Majumdar, A.; Urban, J. J.; Segalman, R. A. Water-processable polymer-nanocrystal hybrids for thermoelectrics. *Nano Lett.* **2010**, *10*, 4664-4667.
- (S17) Bae, E. J.; Kang, Y. H.; Jang, K. S.; Cho, S. Y. Enhancement of Thermoelectric Properties of PEDOT:PSS and Tellurium-PEDOT:PSS Hybrid Composites by Simple Chemical Treatment. *Sci. Rep.* **2016**, *6*, 18805.
- (S18) Moriarty, G. P.; De, S.; King, P. J.; Khan, U.; Via, M.; King, J. A.; Coleman, J. N.; Grunlan, J. C. Thermoelectric behavior of organic thin film nanocomposites. *J. Polym. Sci. Part B: Polym. Phys.* **2013**, *51*, 119-123.
- (S19) Zhang, B.; Sun, J.; Katz, H. E.; Fang, F.; Opila, R. L. Promising thermoelectric properties of commercial PEDOT:PSS materials and their Bi<sub>2</sub>Te<sub>3</sub> powder composites. *ACS Appl. Mater. Inter.* **2010**, *2*, 3170-3178.
- (S20) Yang, Y.; Lin, Z.-H.; Hou, T.; Zhang, F.; Wang, Z. L. Nanowire-composite based flexible thermoelectric nanogenerators and self-powered temperature sensors. *Nano Res.* **2012**, *5*, 888-895.
- (S21) He, M.; Ge, J.; Lin, Z.; Feng, X.; Wang, X.; Lu, H.; Yang, Y.; Qiu, F. Thermopower enhancement in conducting polymer nanocomposites via carrier energy scattering at the organic-inorganic semiconductor interface. *Energ. Environ. Sci.* **2012**, *5*, 8351.

- (S22) Abad, B.; Alda, I.; Díaz-Chao, P.; Kawakami, H.; Almarza, A.; Amantia, D.; Gutierrez, D.; Aubouy, L.; Martín-González, M. Improved power factor of polyaniline nanocomposites with exfoliated graphene nanoplatelets (GNPs). *J. Mater. Chem. A* **2013**, *1*, 10450.
- (S23) Meng, C.; Liu, C.; Fan, S. A promising approach to enhanced thermoelectric properties using carbon nanotube networks. *Adv. Mater.* **2010**, *22*, 535-539.
- (S24) Kim, D.; Kim, Y.; Choi, K.; Grunlan, J. C.; Yu, C. Improved thermoelectric behavior of nanotube-filled polymer composites with poly(3,4-ethylenedioxythiophene) poly(styrenesulfonate). *ACS Nano* **2010**, *4*, 513-523.
- (S25) Prabhakar, R.; Hossain, M. S.; Zheng, W.; Athikam, P. K.; Zhang, Y.; Hsieh, Y.-Y.; Skafidas, E.; Wu, Y.; Shanov, V.; Bahk, J.-H. Tunneling-Limited Thermoelectric Transport in Carbon Nanotube Networks Embedded in Poly(dimethylsiloxane) Elastomer. *ACS Appl. Energ. Mater.* **2019**, *2*, 2419-2426.
- (S26) Yao, Q.; Chen, L.; Zhang, W.; Liufu, S.; Chen, X. Enhanced thermoelectric performance of single-walled carbon nanotubes/polyaniline hybrid nanocomposites. *ACS Nano* **2010**, *4*, 2445-2451.
- (S27) Song, H.; Qiu, Y.; Wang, Y.; Cai, K.; Li, D.; Deng, Y.; He, J. Polymer/carbon nanotube composite materials for flexible thermoelectric power generator. *Compos. Sci. Technol.* **2017**, *153*, 71-83.
- (S28) Liang, L.; Gao, C.; Chen, G.; Guo, C.-Y. Large-area, stretchable, super flexible and mechanically stable thermoelectric films of polymer/carbon nanotube composites. *J. Mater. Chem. C* **2016**, *4*, 526-532.
- (S29) Wang, L.; Yao, Q.; Bi, H.; Huang, F.; Wang, Q.; Chen, L. Large thermoelectric power factor in polyaniline/graphene nanocomposite films prepared by solution-assistant dispersing method. *J. Mater. Chem. A* **2014**, *2*, 11107.
- (S30) Li, F.; Cai, K.; Shen, S.; Chen, S. Preparation and thermoelectric properties of reduced graphene oxide/PEDOT:PSS composite films. *Synthetic Met.* **2014**, *197*, 58-61.

